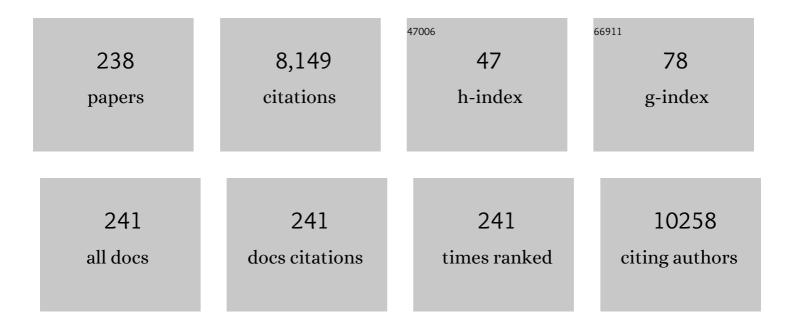
Gianmario Sambuceti

List of Publications by Year in descending order

Source: https://exaly.com/author-pdf/8607598/publications.pdf Version: 2024-02-01



#	Article	IF	CITATIONS
1	Longitudinal analysis of atherosclerotic plaques evolution: an 18F-NaF PET/CT study. Journal of Nuclear Cardiology, 2022, 29, 1713-1723.	2.1	8
2	Functional innervation imaging in the evaluation of cardiotoxicity: Just the beginning of the journey. Journal of Nuclear Cardiology, 2022, 29, 2292-2294.	2.1	1
3	The prognostic power of inflammatory indices and clinical factors in metastatic castration-resistant prostate cancer patients treated with radium-223 (BIO-Ra study). European Journal of Nuclear Medicine and Molecular Imaging, 2022, 49, 1063-1074.	6.4	24
4	18F-FDG-PET correlates of aging and disease course in ALS as revealed by distinct PVC approaches. European Journal of Radiology Open, 2022, 9, 100394.	1.6	1
5	Opportunistic skeletal muscle metrics as prognostic tools in metastatic castration-resistant prostate cancer patients candidates to receive Radium-223. Annals of Nuclear Medicine, 2022, 36, 373-383.	2.2	6
6	Clinical and FDG-PET/CT correlates in patients with polymyalgia rheumatica. Clinical and Experimental Rheumatology, 2022, 40, 78-85.	0.8	7
7	Beyond the Prognostic Value of 2-[18F]FDG PET/CT in Prostate Cancer: A Case Series and Literature Review Focusing on the Diagnostic Value and Impact on Patient Management. Diagnostics, 2022, 12, 581.	2.6	4
8	Prognostic Value of the BIO-Ra Score in Metastatic Castration-Resistant Prostate Cancer Patients Treated with Radium-223 after the European Medicines Agency Restricted Use: Secondary Investigations of the Multicentric BIO-Ra Study. Cancers, 2022, 14, 1744.	3.7	7
9	Mitochondrial Generated Redox Stress Differently Affects the Endoplasmic Reticulum of Circulating Lymphocytes and Monocytes in Treatment-NaÃ⁻ve Hodgkin's Lymphoma. Antioxidants, 2022, 11, 762.	5.1	2
10	Associations among education, age, and the dementia with Lewy bodies (DLB) metabolic pattern: A Europeanâ€ÐLB consortium project. Alzheimer's and Dementia, 2021, 17, 1277-1286.	0.8	5
11	Brain Metabolic Correlates of Persistent Olfactory Dysfunction after SARS-Cov2 Infection. Biomedicines, 2021, 9, 287.	3.2	39
12	18F-fluoro-2-deoxy-d-glucose (FDG) uptake. What are we looking at?. European Journal of Nuclear Medicine and Molecular Imaging, 2021, 48, 1278-1286.	6.4	11
13	The prognostic power of 18F-FDG PET/CT extends to estimating systemic treatment response duration in metastatic castration-resistant prostate cancer (mCRPC) patients. Prostate Cancer and Prostatic Diseases, 2021, 24, 1198-1207.	3.9	24
14	The role of endoplasmic reticulum in in vivo cancer FDG kinetics. PLoS ONE, 2021, 16, e0252422.	2.5	4
15	The Role of the Immune Metabolic Prognostic Index in Patients with Non-Small Cell Lung Cancer (NSCLC) in Radiological Progression during Treatment with Nivolumab. Cancers, 2021, 13, 3117.	3.7	17
16	Two Novel PET Radiopharmaceuticals for Endothelial Vascular Cell Adhesion Molecule-1 (VCAM-1) Targeting. Pharmaceutics, 2021, 13, 1025.	4.5	18
17	Metformin and Cancer Glucose Metabolism: At the Bench or at the Bedside?. Biomolecules, 2021, 11, 1231.	4.0	11
18	Myocardial Metabolic Response Predicts Chemotherapy Curative Potential on Hodgkin Lymphoma: A Proof-of-Concept Study. Biomedicines, 2021, 9, 971.	3.2	1

#	Article	IF	CITATIONS
19	Novel PET Tracers in the Management of Cardiac Sarcoidosis. Current Radiopharmaceuticals, 2021, 14, 220-227.	0.8	1
20	The Role of Endoplasmic Reticulum in the Differential Endurance against Redox Stress in Cortical and Spinal Astrocytes from the Newborn SOD1G93A Mouse Model of Amyotrophic Lateral Sclerosis. Antioxidants, 2021, 10, 1392.	5.1	10
21	Mathematical Models for FDG Kinetics in Cancer: A Review. Metabolites, 2021, 11, 519.	2.9	2
22	Therapeutic efficacy of proton transport inhibitors alone or in combination with cisplatinÂin triple negative and hormone sensitive breast cancer models. Cancer Medicine, 2021, 11, 183.	2.8	4
23	Clinical and FDC-PET/CT correlates in patients with polymyalgia rheumatica. Clinical and Experimental Rheumatology, 2021, , .	0.8	1
24	Spleen Perfusion as an Index of Gender Impact on Sympathetic Nervous System Response to Exercise. Frontiers in Physiology, 2021, 12, 780713.	2.8	1
25	Increased myocardial 18F-FDG uptake as a marker of Doxorubicin-induced oxidative stress. Journal of Nuclear Cardiology, 2020, 27, 2183-2194.	2.1	29
26	Cancer immunotherapy is accompanied by distinct metabolic patterns in primary and secondary lymphoid organs observed by non-invasive <i>in vivo</i> ¹⁸ F-FDG-PET. Theranostics, 2020, 10, 925-937.	10.0	46
27	FDG uptake tracks the oxidative damage in diabetic skeletal muscle: An experimental study. Molecular Metabolism, 2020, 31, 98-108.	6.5	13
28	Comparison Between ¹⁸ F-FDG PET–Based and CT-Based Criteria in Non–Small Cell Lung Cancer Patients Treated with Nivolumab. Journal of Nuclear Medicine, 2020, 61, 990-998.	5.0	44
29	Metabolic Correlates of Dopaminergic Loss in Dementia with Lewy Bodies. Movement Disorders, 2020, 35, 595-605.	3.9	42
30	Role of Baseline and Post-Therapy 18F-FDG PET in the Prognostic Stratification of Metastatic Castration-Resistant Prostate Cancer (mCRPC) Patients Treated with Radium-223. Cancers, 2020, 12, 31.	3.7	30
31	Mathematical modelling of nuclear medicine data. , 2020, , .		3
32	Two high-rate pentose-phosphate pathways in cancer cells. Scientific Reports, 2020, 10, 22111.	3.3	19
33	The Prognostic Role of Baseline Metabolic Tumor Burden and Systemic Inflammation Biomarkers in Metastatic Castration-Resistant Prostate Cancer Patients Treated with Radium-223: A Proof of Concept Study. Cancers, 2020, 12, 3213.	3.7	22
34	18F-Fluorodeoxyglucose Positron Emission Tomography Tracks the Heterogeneous Brain Susceptibility to the Hyperglycemia-Related Redox Stress. International Journal of Molecular Sciences, 2020, 21, 8154.	4.1	6
35	Spinal cord hypermetabolism extends to skeletal muscle in amyotrophic lateral sclerosis: a computational approach to [18F]-fluorodeoxyglucose PET/CT images. EJNMMI Research, 2020, 10, 23.	2.5	17
36	Subretinally injected semiconducting polymer nanoparticles rescue vision in a rat model of retinal dystrophy. Nature Nanotechnology, 2020, 15, 698-708.	31.5	129

#	Article	IF	CITATIONS
37	Editorial: Perspectives in Small Animal Radionuclide Imaging. Frontiers in Medicine, 2020, 7, 262.	2.6	2
38	Insulin-independent stimulation of skeletal muscle glucose uptake by low-dose abscisic acid via AMPK activation. Scientific Reports, 2020, 10, 1454.	3.3	20
39	The Elusive Link Between Cancer FDG Uptake and Glycolytic Flux Explains the Preserved Diagnostic Accuracy of PET/CT in Diabetes. Translational Oncology, 2020, 13, 100752.	3.7	8
40	Mechanisms underlying the predictive power of high skeletal muscle uptake of FDG in amyotrophic lateral sclerosis. EJNMMI Research, 2020, 10, 76.	2,5	15
41	Anthropometric and glucometabolic changes in an aged mouse model of lipocalin-2 overexpression. International Journal of Obesity, 2019, 43, 189-201.	3.4	9
42	Radionuclide Imaging of Cardiovascular Disease. , 2019, , 449-497.		0
43	Automated Definition of Skeletal Disease Burden in Metastatic Prostate Carcinoma: A 3D Analysis of SPECT/CT Images. Cancers, 2019, 11, 869.	3.7	1
44	Molecular imaging of multiple sclerosis: from the clinical demand to novel radiotracers. EJNMMI Radiopharmacy and Chemistry, 2019, 4, 6.	3.9	29
45	Metabolic patterns across core features in dementia with lewy bodies. Annals of Neurology, 2019, 85, 715-725.	5.3	47
46	Head-to-Head Comparison among Semi-Quantification Tools of Brain FDG-PET to Aid the Diagnosis of Prodromal Alzheimer's Disease1. Journal of Alzheimer's Disease, 2019, 68, 383-394.	2.6	14
47	G6Pase location in the endoplasmic reticulum: Implications on compartmental analysis of FDG uptake in cancer cells. Scientific Reports, 2019, 9, 2794.	3.3	22
48	FDG-PET Imaging of Doxorubicin-Induced Cardiotoxicity: a New Window on an Old Problem. Current Cardiovascular Imaging Reports, 2019, 12, 1.	0.6	5
49	Neuroimaging findings and clinical trajectories of Lewy body disease in patients with MCI. Neurobiology of Aging, 2019, 76, 9-17.	3.1	23
50	Procedural Recommendations for Lymphoscintigraphy in the Diagnosis of Peripheral Lymphedema: the Genoa Protocol. Nuclear Medicine and Molecular Imaging, 2019, 53, 47-56.	1.0	22
51	Obligatory role of endoplasmic reticulum in brain FDG uptake. European Journal of Nuclear Medicine and Molecular Imaging, 2019, 46, 1184-1196.	6.4	24
52	The Metabolic Pattern of Idiopathic REM Sleep Behavior Disorder Reflects Early-Stage Parkinson Disease. Journal of Nuclear Medicine, 2018, 59, 1437-1444.	5.0	80
53	Reference Tissue Models for FDG-PET Data: Identifiability and Solvability. IEEE Transactions on Radiation and Plasma Medical Sciences, 2018, 2, 177-186.	3.7	9
54	Reply: Doxorubicin Effect on Myocardial Metabolism as a Prerequisite for Subsequent Development of Cardiac Toxicity: Are There Unsuspected Confounders?. Journal of Nuclear Medicine, 2018, 59, 713.2-714.	5.0	1

#	Article	IF	CITATIONS
55	Metabolic correlates of reserve and resilience in MCI due to Alzheimer's Disease (AD). Alzheimer's Research and Therapy, 2018, 10, 35.	6.2	22
56	Small-Animal 18F-FDG PET for Research on Octopus vulgaris: Applications and Future Directions in Invertebrate Neuroscience and Tissue Regeneration. Journal of Nuclear Medicine, 2018, 59, 1302-1307.	5.0	12
57	Prevention of systemic toxicity in hyperthermic isolated lung perfusion using radioisotopic leakage monitoring. International Journal of Hyperthermia, 2018, 34, 469-478.	2.5	1
58	Effect of starvation on brain glucose metabolism and 18F-2-fluoro-2-deoxyglucose uptake: an experimental in-vivo and ex-vivo study. EJNMMI Research, 2018, 8, 44.	2.5	14
59	Enhancement of Tumor Homing by Chemotherapy‣oaded Nanoparticles. Small, 2018, 14, e1802886.	10.0	23
60	An increase in myocardial 18-fluorodeoxyglucose uptake is associated with left ventricular ejection fraction decline in Hodgkin lymphoma patients treated with anthracycline. Journal of Translational Medicine, 2018, 16, 295.	4.4	43
61	Interplay between spinal cord and cerebral cortex metabolism in amyotrophic lateral sclerosis. Brain, 2018, 141, 2272-2279.	7.6	33
62	Assessment of Skeletal Tumor Load in Metastasized Castration-Resistant Prostate Cancer Patients: A Review of Available Methods and an Overview on Future Perspectives. Bioengineering, 2018, 5, 58.	3.5	3
63	Metabolic and densitometric correlation between atherosclerotic plaque and trabecular bone: an F-Natrium-Fluoride PET/CT study. American Journal of Nuclear Medicine and Molecular Imaging, 2018, 8, 387-396.	1.0	2
64	Comparison of coronary flow reserve estimated by dynamic radionuclide SPECT and multi-detector x-ray CT. Journal of Nuclear Cardiology, 2017, 24, 1712-1721.	2.1	10
65	Progressive Disintegration of Brain Networking from Normal Aging to Alzheimer Disease: Analysis of Independent Components of ¹⁸ F-FDG PET Data. Journal of Nuclear Medicine, 2017, 58, 1132-1139.	5.0	41
66	A fully organic retinal prosthesis restores vision in a rat model of degenerative blindness. Nature Materials, 2017, 16, 681-689.	27.5	232
67	Circulating Tumor DNA Reflects Tumor Metabolism Rather Than Tumor Burden in Chemotherapy-Naive Patients with Advanced Non–Small Cell Lung Cancer: ¹⁸ F-FDG PET/CT Study. Journal of Nuclear Medicine, 2017, 58, 1764-1769.	5.0	44
68	MA10.09 Comparison between CT Scan Evaluation Criteria and PERCIST for Evaluation of Immune Check-Point Inhibitors Response. Journal of Thoracic Oncology, 2017, 12, S401-S402.	1.1	0
69	Radionuclide imaging of subendocardial ischaemia: an insight into coronary pathophysiology or a technical artefact?. European Journal of Nuclear Medicine and Molecular Imaging, 2017, 44, 861-865.	6.4	1
70	¹⁸ F-Fluorodeoxyglucose Imaging of Inflammation. Circulation: Cardiovascular Imaging, 2017, 10, e006185.	2.6	2
71	Abscisic acid enhances glucose disposal and induces brown fat activity in adipocytes in vitro and in vivo. Biochimica Et Biophysica Acta - Molecular and Cell Biology of Lipids, 2017, 1862, 131-144.	2.4	32
72	Functional Activation of Osteoclast Commitment in Chronic Lymphocytic Leukaemia: a Possible Role for RANK/RANKL Pathway. Scientific Reports, 2017, 7, 14159.	3.3	14

#	Article	IF	CITATIONS
73	A physiology-based parametric imaging method for FDG–PET data. Inverse Problems, 2017, 33, 125010.	2.0	12
74	The Alzheimer's disease metabolic brain pattern in mild cognitive impairment. Journal of Cerebral Blood Flow and Metabolism, 2017, 37, 3643-3648.	4.3	29
75	18F–FDG PET diagnostic and prognostic patterns do not overlap in Alzheimer's disease (AD) patients at the mild cognitive impairment (MCI) stage. European Journal of Nuclear Medicine and Molecular Imaging, 2017, 44, 2073-2083.	6.4	29
76	Prediction of cognitive worsening in de novo Parkinson's disease: Clinical use of biomarkers. Movement Disorders, 2017, 32, 1738-1747.	3.9	43
77	Doxorubicin Effect on Myocardial Metabolism as a Prerequisite for Subsequent Development of Cardiac Toxicity: A Translational ¹⁸ F-FDG PET/CT Observation. Journal of Nuclear Medicine, 2017, 58, 1638-1645.	5.0	65
78	Early identification of MCI converting to AD: a FDG PET study. European Journal of Nuclear Medicine and Molecular Imaging, 2017, 44, 2042-2052.	6.4	83
79	Relationship between circulating anti-thyroglobulin antibodies (TgAb) and tumor metabolism in patients with differentiated thyroid cancer (DTC): prognostic implications. Journal of Endocrinological Investigation, 2017, 40, 417-424.	3.3	18
80	A Score-Based Approach to 18F-FDG PET Images as a Tool to Describe Metabolic Predictors of Myocardial Doxorubicin Susceptibility. Diagnostics, 2017, 7, 57.	2.6	11
81	Tumor Burden and Intraosseous Metabolic Activity as Predictors of Bone Marrow Failure during Radioisotope Therapy in Metastasized Prostate Cancer Patients. BioMed Research International, 2017, 2017, 1-10.	1.9	12
82	Comparative diagnostic accuracy of ¹⁸ F-FDG PET/CT for breast cancer recurrence. Breast Cancer: Targets and Therapy, 2017, Volume 9, 461-471.	1.8	12
83	Evaluation of response to immune checkpoint inhibitors: Is there a role for positron emission tomography?. World Journal of Radiology, 2017, 9, 27.	1.1	17
84	Cardiac and aortic involvement in patients with polymyalgia rheumatica: a study with echocardiography and FDG-PET/CT. Clinical and Experimental Rheumatology, 2017, 35 Suppl 103, 224.	0.8	1
85	Diagnostic value of ischemia severity at myocardial perfusion imaging in elderly persons with suspected coronary disease. Journal of Cardiovascular Medicine, 2016, 17, 719-728.	1.5	4
86	Mapping brain morphological and functional conversion patterns in predementia late-onset bvFTD. European Journal of Nuclear Medicine and Molecular Imaging, 2016, 43, 1337-1347.	6.4	27
87	Multicentre multi-device hybrid imaging study of coronary artery disease: results from the EValuation of INtegrated Cardiac Imaging for the Detection and Characterization of Ischaemic Heart Disease (EVINCI) hybrid imaging population. European Heart Journal Cardiovascular Imaging, 2016, 17, 951-960.	1.2	95
88	Predicting the transition from normal aging to Alzheimer's disease: A statistical mechanistic evaluation of FDG-PET data. NeuroImage, 2016, 141, 282-290.	4.2	36
89	A PET/CT approach to spinal cord metabolism in amyotrophic lateral sclerosis. European Journal of Nuclear Medicine and Molecular Imaging, 2016, 43, 2061-2071.	6.4	27
90	Discovery of a novel glucose metabolism in cancer: The role of endoplasmic reticulum beyond glycolysis and pentose phosphate shunt. Scientific Reports, 2016, 6, 25092.	3.3	67

#	Article	IF	CITATIONS
91	Divergent targets of glycolysis and oxidative phosphorylation result in additive effects of metformin and starvation in colon and breast cancer. Scientific Reports, 2016, 6, 19569.	3.3	43
92	HT-BONE: a graphical user interface for the identification of bone profiles in CT images via extended Hough transform. , 2016, , .		3
93	Positive PET in a Patient With Esophageal Leiomyoma. American Journal of Gastroenterology, 2016, 111, 767.	0.4	4
94	A mathematical model for the vessel recruitment in coronary microcirculation in the absence of active autoregulation. Microvascular Research, 2016, 104, 38-45.	2.5	1
95	Baseline and ongoing PET-derived factors predict detrimental effect or potential utility of 18F-FDG PET/CT (FDG-PET/CT) performed for surveillance in asymptomatic lymphoma patients in first remission. European Journal of Nuclear Medicine and Molecular Imaging, 2016, 43, 232-239.	6.4	9
96	Correlation between thoracic aorta 18F-natrium fluoride uptake and cardiovascular risk. World Journal of Radiology, 2016, 8, 82.	1.1	15
97	Comparisons between glucose analogue 2-deoxy-2-(¹⁸ F)fluoro-D-glucose and ¹⁸ F-sodium fluoride positron emission tomography/computed tomography in breast cancer patients with bone lesions. World Journal of Radiology, 2016, 8, 200.	1.1	13
98	Sequential use of vinorelbine followed by gefitinib enhances the antitumor effect in <scp>NSCLC</scp> cell lines poorly responsive to reversible <scp>EGFR</scp> tyrosine kinase inhibitors. International Journal of Cancer, 2015, 137, 2947-2958.	5.1	11
99	A new compartmental method for the analysis of liver FDG kinetics in small animal models. EJNMMI Research, 2015, 5, 107.	2.5	19
100	The Role of the Serotonergic System in REM Sleep Behavior Disorder. Sleep, 2015, 38, 1505-1509.	1.1	36
101	Cardiac resynchronization therapy and cardiac sympathetic function. European Journal of Clinical Investigation, 2015, 45, 792-799.	3.4	18
102	Fasting induces anti-Warburg effect that increases respiration but reduces ATP-synthesis to promote apoptosis in colon cancer models. Oncotarget, 2015, 6, 11806-11819.	1.8	127
103	IGF1 regulates PKM2 function through Akt phosphorylation. Cell Cycle, 2015, 14, 1559-1567.	2.6	42
104	A New Integrated Clinical-Biohumoral Model to PredictÂFunctionally Significant Coronary Artery Disease inÂPatients With Chronic Chest Pain. Canadian Journal of Cardiology, 2015, 31, 709-716.	1.7	19
105	¹⁸ F-NaF Uptake by Atherosclerotic Plaque on PET/CT Imaging: Inverse Correlation Between Calcification Density and Mineral Metabolic Activity. Journal of Nuclear Medicine, 2015, 56, 1019-1023.	5.0	73
106	Volume of interest-based [18F]fluorodeoxyglucose PET discriminates MCI converting to Alzheimer's disease from healthy controls. A European Alzheimer's Disease Consortium (EADC) study. NeuroImage: Clinical, 2015, 7, 34-42.	2.7	85
107	Detection of Significant Coronary Artery Disease by Noninvasive Anatomical and Functional Imaging. Circulation: Cardiovascular Imaging, 2015, 8, .	2.6	286
108	Neuroblastoma-targeted nanocarriers improve drug delivery and penetration, delay tumor growth and abrogate metastatic diffusion. Biomaterials, 2015, 68, 89-99.	11.4	36

#	Article	IF	CITATIONS
109	Added prognostic value of ischaemic threshold in radionuclide myocardial perfusion imaging: a common-sense integration of exercise tolerance and ischaemia severity. European Journal of Nuclear Medicine and Molecular Imaging, 2015, 42, 750-760.	6.4	5
110	Allogeneic cell transplant expands bone marrow distribution by colonizing previously abandoned areas: an FDG PET/CT analysis. Blood, 2015, 125, 4095-4102.	1.4	23
111	Role of [18F]Fluorodeoxyglucose Positron Emission Tomography-Computed Tomography for Diagnosis and Treatment of Sarcoidosis in an HIV-2-Infected Patient. AIDS Research and Human Retroviruses, 2015, 31, 868-869.	1.1	0
112	Nigro-caudate dopaminergic deafferentation: a marker of REM sleep behavior disorder?. Neurobiology of Aging, 2015, 36, 3300-3305.	3.1	63
113	Pathophysiological basis of myocardial innervation imaging in heart failure. Clinical and Translational Imaging, 2015, 3, 347-355.	2.1	3
114	Heterogeneous response of cardiac sympathetic function to cardiac resynchronization therapy in heart failure documented by 11[C]-hydroxy-ephedrine and PET/CT. Nuclear Medicine and Biology, 2015, 42, 858-863.	0.6	11
115	Visual Versus Semi-Quantitative Analysis of 18F-FDG-PET in Amnestic MCI: An European Alzheimer's Disease Consortium (EADC) Project. Journal of Alzheimer's Disease, 2015, 44, 815-826.	2.6	67
116	Metformin inhibits cell cycle progression of B-cell chronic lymphocytic leukemia cells. Oncotarget, 2015, 6, 22624-22640.	1.8	30
117	Diagnostic and prognostic value of 18F-FDG PET/CT in comparison with morphological imaging in primary adrenal gland malignancies - a multicenter experience. Hellenic Journal of Nuclear Medicine, 2015, 18, 97-102.	0.3	24
118	18F-FDG PET/CT is a prognostic biomarker in patients affected by bone metastases from breast cancer in comparison with 18F-NaF PET/CT. Nuklearmedizin - NuclearMedicine, 2015, 54, 163-172.	0.7	18
119	Metformin and cancer: Technical and clinical implications for FDG-PET imaging. World Journal of Radiology, 2015, 7, 57.	1.1	10
120	18F-fluorodeoxyglucose PET/CT in aplastic anemia: a literature review and the potential of a computational approach. Clinical Practice (London, England), 2014, 11, 613-621.	0.1	4
121	Interspinous bursitis is common in polymyalgia rheumatica, but is not associated with spinal pain. Arthritis Research and Therapy, 2014, 16, 492.	3.5	30
122	Efficacy of sorafenib and impact on cardiac function in patients with thyroid cancer: a retrospective analysis. Journal of Endocrinological Investigation, 2014, 37, 1099-1108.	3.3	3
123	Adult Advanced Chronic Lymphocytic Leukemia: Computational Analysis of Whole-Body CT Documents a Bone Structure Alteration. Radiology, 2014, 271, 805-813.	7.3	24
124	Polymyalgia rheumatica or lymphoma recurrence? Positron emission tomography/computed tomography is a specific imaging technique that helps differential diagnosis. Rheumatology, 2014, 53, 809-809.	1.9	0
125	Nuclear Cardiology in Heart Failure. Current Cardiovascular Imaging Reports, 2014, 7, 1.	0.6	1
126	Divergent determinants of 18F–NaF uptake and visible calcium deposition in large arteries: relationship with Framingham risk score. International Journal of Cardiovascular Imaging, 2014, 30, 439-447.	1.5	47

#	Article	IF	CITATIONS
127	A novel description of FDG excretion in the renal system: application to metformin-treated models. Physics in Medicine and Biology, 2014, 59, 2469-2484.	3.0	20
128	Implementation strategies of Systems Medicine in clinical research and home care for cardiovascular disease patients. European Journal of Internal Medicine, 2014, 25, 785-794.	2.2	9
129	Metformin, cancer and glucose metabolism. Endocrine-Related Cancer, 2014, 21, R461-R471.	3.1	91
130	Contrast-enhanced [18 F] fluorodeoxyglucose-positron emission tomography/computed tomography in clinical oncology: tumor-, site-, and question-based comparison with standard positron emission tomography/computed tomography. Cancer Imaging, 2014, 14, 10.	2.8	10
131	Metabolic Correlates of Rey Auditory Verbal Learning Test in Elderly Subjects with Memory Complaints. Journal of Alzheimer's Disease, 2014, 39, 103-113.	2.6	39
132	¹¹ C-mHED for PET / CT: Principles of Synthesis, Methodology and First Clinical Applications. Current Radiopharmaceuticals, 2014, 7, 79-83.	0.8	5
133	Microalbuminuria predicts silent myocardial ischaemia in type 2 diabetes patients. European Journal of Nuclear Medicine and Molecular Imaging, 2013, 40, 548-557.	6.4	13
134	1,25-Dihydroxy vitamin D and coronary microvascular function. European Journal of Nuclear Medicine and Molecular Imaging, 2013, 40, 280-289.	6.4	9
135	Tissue specificity in fasting glucose utilization in slightly obese diabetic patients submitted to bariatric surgery. Obesity, 2013, 21, E175-81.	3.0	8
136	An optimisation approach to multiprobe cryosurgery planning. Computer Methods in Biomechanics and Biomedical Engineering, 2013, 16, 885-895.	1.6	21
137	Comparison of Sulfur Hexafluoride Microbubble (SonoVue)-Enhanced Myocardial Contrast Echocardiography With Gated Single-Photon Emission Computed Tomography for Detection of Significant Coronary Artery Disease. Journal of the American College of Cardiology, 2013, 62, 1353-1361.	2.8	97
138	Metformin selectively affects human glioblastoma tumor-initiating cell viability. Cell Cycle, 2013, 12, 145-156.	2.6	154
139	Metabolic Networks Underlying Cognitive Reserve in Prodromal Alzheimer Disease: A European Alzheimer Disease Consortium Project. Journal of Nuclear Medicine, 2013, 54, 894-902.	5.0	108
140	Metformin Temporal and Localized Effects on Gut Glucose Metabolism Assessed Using ¹⁸ F-FDG PET in Mice. Journal of Nuclear Medicine, 2013, 54, 259-266.	5.0	50
141	High frequency of capsular knee involvement in polymyalgia rheumatica/giant cell arteritis patients studied by positron emission tomography. Rheumatology, 2013, 52, 1865-1872.	1.9	35
142	Pattern recognition in medical imaging by means of the Hough transform of curves. , 2013, , .		4
143	Direct inhibition of hexokinase activity by metformin at least partially impairs glucose metabolism and tumor growth in experimental breast cancer. Cell Cycle, 2013, 12, 3490-3499.	2.6	124
144	Metformin Impairs Glucose Consumption and Survival in Calu-1 Cells by Direct Inhibition of Hexokinase-II. Scientific Reports, 2013, 3, 2070.	3.3	100

#	Article	IF	CITATIONS
145	CD16 ⁺ Monocyte Subsets Are Increased in Large Abdominal Aortic Aneurysms and Are Differentially Related with Circulating and Cell-Associated Biochemical and Inflammatory Biomarkers. Disease Markers, 2013, 34, 131-142.	1.3	34
146	Estimate of FDG Excretion by means of Compartmental Analysis and Ant Colony Optimization of Nuclear Medicine Data. Computational and Mathematical Methods in Medicine, 2013, 2013, 1-10.	1.3	10
147	Use of the Uteroglobin Platform for the Expression of a Bivalent Antibody against Oncofetal Fibronectin in Escherichia coli. PLoS ONE, 2013, 8, e82878.	2.5	0
148	Intrabone Transplant of Cord Blood Stem Cells Establishes a Local Engraftment Store: A Functional PET/FDG Study. Journal of Biomedicine and Biotechnology, 2012, 2012, 1-8.	3.0	8
149	A Positron Emission Tomography/Computed Tomography (PET/CT) Evaluation of Asymptomatic Abdominal Aortic Aneurysms: Another Point of View. Annals of Vascular Surgery, 2012, 26, 491-499.	0.9	35
150	What predicts cognitive decline in de novo Parkinson's disease?. Neurobiology of Aging, 2012, 33, 1127.e11-1127.e20.	3.1	34
151	Resting metabolic connectivity in prodromal Alzheimer's disease. A European Alzheimer Disease Consortium (EADC) project. Neurobiology of Aging, 2012, 33, 2533-2550.	3.1	108
152	Estimating the whole bone-marrow asset in humans by a computational approach to integrated PET/CT imaging. European Journal of Nuclear Medicine and Molecular Imaging, 2012, 39, 1326-1338.	6.4	51
153	Direct relationship between cell density and FDG uptake in asymptomatic aortic aneurysm close to surgical threshold: an in vivo and in vitro study. European Journal of Nuclear Medicine and Molecular Imaging, 2012, 39, 91-101.	6.4	29
154	Radionuclide brain imaging correlates of cognitive impairment in Parkinson's disease (PD). Journal of the Neurological Sciences, 2011, 310, 31-35.	0.6	19
155	Brain perfusion correlates of cognitive and nigrostriatal functions in de novo Parkinson's disease. European Journal of Nuclear Medicine and Molecular Imaging, 2011, 38, 2209-2218.	6.4	32
156	Mesenchymal stem cells impair in vivo T-cell priming by dendritic cells. Proceedings of the National Academy of Sciences of the United States of America, 2011, 108, 17384-17389.	7.1	241
157	Structural Abnormalities of the Coronary Arterial Wall—in Addition to Luminal Narrowing—Affect Myocardial Blood Flow Reserve. Journal of Nuclear Medicine, 2011, 52, 1704-1712.	5.0	48
158	Cardiac computed tomography and myocardial perfusion scintigraphy for risk stratification in asymptomatic individuals without known cardiovascular disease: a position statement of the Working Group on Nuclear Cardiology and Cardiac CT of the European Society of Cardiology. European Heart Journal, 2011, 32, 1986-1993.	2.2	122
159	Whole Body and Cardiac Metaiodobenzylguanidine Kinetics in Parkinson Disease and Multiple System Atrophy. Clinical Nuclear Medicine, 2010, 35, 311-316.	1.3	7
160	Unawareness of Memory Deficit in Amnestic MCI: FDG-PET Findings. Journal of Alzheimer's Disease, 2010, 22, 993-1003.	2.6	59
161	Optimization of flow reserve measurement using SPECT technology to evaluate the determinants of coronary microvascular dysfunction in diabetes. European Journal of Nuclear Medicine and Molecular Imaging, 2010, 37, 357-367.	6.4	17
162	Reduced coronary flow reserve in patients with primary hyperparathyroidism: a study by G-SPECT myocardial perfusion imaging. European Journal of Nuclear Medicine and Molecular Imaging, 2010, 37, 2256-2263.	6.4	28

#	Article	IF	CITATIONS
163	Contact with the bone marrow microenvironment readdresses the fate of transplanted hematopoietic stem cells. Experimental Hematology, 2010, 38, 968-977.	0.4	21
164	Improved myocardial perfusion in chronic diabetic mice by the upâ€regulation of pLKB1 and AMPK signaling. Journal of Cellular Biochemistry, 2010, 109, 1033-1044.	2.6	32
165	Cognitiveâ€nigrostriatal relationships in de novo, drugâ€naÃ⁻ve Parkinson's disease patients: A [lâ€123]FP IT SPECT study. Movement Disorders, 2010, 25, 35-43.	3.9	83
166	The Reversed Clock Drawing Test Phenomenon in Alzheimer's Disease: A Perfusion SPECT Study. Dementia and Geriatric Cognitive Disorders, 2010, 29, 1-10.	1.5	8
167	The intra-bone marrow injection of cord blood cells extends the possibility of transplantation to the majority of patients with malignant hematopoietic diseases. Best Practice and Research in Clinical Haematology, 2010, 23, 237-244.	1.7	29
168	Amnestic mild cognitive impairment in Parkinson's disease: A brain perfusion SPECT study. Movement Disorders, 2009, 24, 414-421.	3.9	63
169	Clinical images: The multifaceted pathogenesis of polymyalgia rheumatica/giant cell arteritis. Arthritis and Rheumatism, 2009, 60, 2771-2771.	6.7	9
170	Witnessing ischemia or proofing coronary atherosclerosis: two different windows on the same or on different pathways precipitating cardiovascular events?. Journal of Nuclear Cardiology, 2009, 16, 447-455.	2.1	3
171	Assessing the need for nuclear cardiology and other advanced cardiac imaging modalities in the developing world. Journal of Nuclear Cardiology, 2009, 16, 956-961.	2.1	64
172	Diabetes Impairs the Vascular Recruitment of Normal Stem Cells by Oxidant Damage, Reversed by Increases in pAMPK, Heme Oxygenase-1, and Adiponectin. Stem Cells, 2009, 27, 399-407.	3.2	75
173	The Intra-Bone Route of Administration of Cord blood cells extends the Possibility of Transplantation to the Majority of Patients with Malignant Hematopoietic Diseases Blood, 2009, 114, 3376-3376.	1.4	1
174	I-123-mIBG myocardial imaging for assessment of risk for a major cardiac event in heart failure patients: insights from a retrospective European multicenter study. European Journal of Nuclear Medicine and Molecular Imaging, 2008, 35, 535-546.	6.4	199
175	Reply: High Intraindividual Variability of Global Myocardial 18F-FDG Uptake over Time. Journal of Nuclear Medicine, 2008, 49, 1570.2-1571.	5.0	0
176	Whole-Body Evaluation of MIBG Tissue Extraction in a Mouse Model of Long-Lasting Type II Diabetes and Its Relationship with Norepinephrine Transport Protein Concentration. Journal of Nuclear Medicine, 2008, 49, 1701-1706.	5.0	13
177	<i>In Vivo</i> Imaging Shows Abnormal Function of Vascular Endothelial Growth Factor-Induced Vasculature. Human Gene Therapy, 2007, 18, 515-524.	2.7	66
178	Spatial and Temporal Heterogeneity of Regional Myocardial Uptake in Patients Without Heart Disease Under Fasting Conditions on Repeated Whole-Body 18F-FDG PET/CT. Journal of Nuclear Medicine, 2007, 48, 1662-1669.	5.0	83
179	Recombinant P-selectin glycoprotein ligand–immunoglobulin, a P-selectin antagonist, as an adjunct to thrombolysis in acute myocardial infarction. The P-Selectin Antagonist Limiting Myonecrosis (PSALM) trial. American Heart Journal, 2006, 152, 125.e1-125.e8.	2.7	42
180	Paradoxical coronary microcirculatory constriction during ischemia: a synergic function for nitric oxide and endothelin. American Journal of Physiology - Heart and Circulatory Physiology, 2006, 291, H1814-H1821.	3.2	14

#	Article	IF	CITATIONS
181	Migraine during systemic lupus erythematosus: findings from brain single photon emission computed tomography. Journal of Rheumatology, 2006, 33, 2184-91.	2.0	5
182	Extension of myocardial necrosis differently affects MIBG retention in heart failure caused by ischaemic heart disease or by dilated cardiomyopathy. European Journal of Nuclear Medicine and Molecular Imaging, 2005, 32, 682-688.	6.4	23
183	Differences and similarities between coronary atherosclerosis and ischaemic heart disease: implications for cardiac imaging. European Journal of Nuclear Medicine and Molecular Imaging, 2005, 32, 385-388.	6.4	4
184	Coronary microcirculatory vasoconstriction is heterogeneously distributed in acutely ischemic myocardium. American Journal of Physiology - Heart and Circulatory Physiology, 2005, 288, H2298-H2305.	3.2	27
185	Baseline/post-nitrate Tc-99m tetrofosmin mismatch for the assessment of myocardial viability in patients with severe left ventricular dysfunction: comparison with baseline Tc-99m tetrofosmin scintigraphy/FDC PET imaging. Journal of Nuclear Cardiology, 2004, 11, 142-151.	2.1	18
186	Revascularization of dysfunctioning myocardium: differential prognostic effects of coronary artery bypass grafting and percutaneous transluminal coronary angioplasty in patients with three-vessel disease and mostly viable myocardium. Interactive Cardiovascular and Thoracic Surgery, 2003, 2, 301-306.	1.1	0
187	Prognostic Role of Myocardial Blood Flow Impairment in Idiopathic Left Ventricular Dysfunction. Circulation, 2002, 105, 186-193.	1.6	401
188	Platelet glycoprotein IIb/IIIa receptor blockade and coronary resistance in unstable angina. Journal of the American College of Cardiology, 2002, 40, 2102-2109.	2.8	32
189	Myocardial metabolic and receptor imaging in idiopathic dilated cardiomyopathy. European Journal of Nuclear Medicine and Molecular Imaging, 2002, 29, 1403-1413.	6.4	17
190	Cardiac phantom measurement validating the methodology for a cardiac multi-centre trial with positron emission tomography. European Journal of Nuclear Medicine and Molecular Imaging, 2002, 29, 1588-1593.	6.4	8
191	Myocardial perfusion and coronary microcirculation: From pathophysiology to clinical application. Journal of Nuclear Cardiology, 2002, 9, 328-337.	2.1	15
192	Microcirculatory Function: Coronary Vasculature. , 2002, , 162-174.		0
193	Significance of both negative T waves and stress-induced normalization of the repolarization phase in infarcted patients: a positron-emission-tomography assessment of regulation of myocardial blood flow and viability of myocardium. Coronary Artery Disease, 2001, 12, 205-215.	0.7	5
194	Studying the neuronal side of the synaptic cleft. A tool for investigating the paradox of sympathetic nervous system and heart failure in dilated cardiomyopathy. European Heart Journal, 2001, 22, 1521-1522.	2.2	2
195	Paradoxical Increase in Microvascular Resistance During Tachycardia Downstream From a Severe Stenosis in Patients With Coronary Artery Disease. Circulation, 2001, 103, 2352-2360.	1.6	71
196	Clinical evidence for myocardial derecruitment downstream from severe stenosis: pressure-flow control interaction. American Journal of Physiology - Heart and Circulatory Physiology, 2000, 279, H2641-H2648.	3.2	10
197	Why should we study the coronary microcirculation?. American Journal of Physiology - Heart and Circulatory Physiology, 2000, 279, H2581-H2584.	3.2	19
198	Coronary microcirculatory vasoconstriction during ischemia in patients with unstable angina. Journal of the American College of Cardiology, 2000, 35, 327-334.	2.8	71

#	Article	IF	CITATIONS
199	Effects of Long-term Treatment with Verapamil on Left Ventricular Function and Myocardial Blood Flow in Patients with Dilated Cardiomyopathy Without Overt Heart Failure. Journal of Cardiovascular Pharmacology, 2000, 36, 744-750.	1.9	18
200	Methods for evaluating coronary microvasculature in humans. European Heart Journal, 1999, 20, 1300-1313.	2.2	23
201	Myocardial blood flow and perfusion reserve in infarcted patients with stress-induced normalization of previously negative T waves: A positron emission tomography study. Journal of Nuclear Cardiology, 1999, 6, 11-19.	2.1	5
202	High dose dipyridamole myocardial imaging: simultaneous sestamibi scintigraphy and two-dimensional echocardiography in the detection and evaluation of coronary artery disease. Coronary Artery Disease, 1999, 10, 177-184.	0.7	20
203	Evaluation of compartmental and spectral analysis models of [/sup 18/F]FDG kinetics for heart and brain studies with PET. IEEE Transactions on Biomedical Engineering, 1998, 45, 1429-1448.	4.2	55
204	Homogeneously Reduced Versus Regionally Impaired Myocardial Blood Flow in Hypertensive Patients: Two Different Patterns of Myocardial Perfusion Associated With Degree of Hypertrophy. Journal of the American College of Cardiology, 1998, 31, 366-373.	2.8	76
205	Myocardial and forearm blood flow reserve in mild-moderate essential hypertensive patients. Journal of Hypertension, 1997, 15, 667-673.	0.5	23
206	Correlation between extent of myocardial dysfunction and markers of irreversible damage in failing hearts1, 2. Journal of Nuclear Cardiology, 1997, 4, 441-450.	2.1	1
207	Coronary Vasoconstriction During Myocardial Ischemia Induced by Rises in Metabolic Demand in Patients With Coronary Artery Disease. Circulation, 1997, 95, 2652-2659.	1.6	86
208	Comparative Effects of Enalapril and Verapamil on Myocardial Blood Flow in Systemic Hypertension. Circulation, 1997, 96, 864-873.	1.6	65
209	Improvement of Hibernation in the Clinical Setting. Journal of Molecular and Cellular Cardiology, 1996, 28, 2415-2418.	1.9	9
210	No relationship between maximum coronary flow and resistance and left ventricular mass in essential hypertension. Journal of the American College of Cardiology, 1996, 27, 105-106.	2.8	1
211	Morphological bases for thallium-201 uptake in cardiac imaging and correlates with myocardial blood flow distribution. European Heart Journal, 1996, 17, 951-961.	2.2	9
212	Perfusional and metabolic effects of nisoldipine as shown by positron emission tomography after acute myocardial infarction. American Journal of Cardiology, 1995, 75, E31-E35.	1.6	7
213	Regional concordance and discordance between rest thallium 201 and sestamibi imaging for assessing tissue viability: Comparison with postrevascularization functional recovery+. Journal of Nuclear Cardiology, 1995, 2, 309-316.	2.1	28
214	Role of coronary microvascular abnormalities in coronary artery disease—implications for perfusion imaging. Journal of Nuclear Cardiology, 1995, 2, 78-84.	2.1	4
215	Myocardial Viability: Nuclear Medicine Versus Stress Echocardiography. Echocardiography, 1995, 12, 291-302.	0.9	7
216	Microvascular dysfunction in collateral-dependent myocardium. Journal of the American College of Cardiology, 1995, 26, 615-623.	2.8	56

#	Article	IF	CITATIONS
217	Residual coronary reserve identifies segmental viability in patients with wall motion abnormalities. Journal of the American College of Cardiology, 1995, 26, 342-350.	2.8	49
218	Myocardial Blood Flow Response to Pacing Tachycardia and to Dipyridamole Infusion in Patients With Dilated Cardiomyopathy Without Overt Heart Failure. Circulation, 1995, 92, 796-804.	1.6	184
219	Assessment of anatomic and physiological severity of single-vessel coronary artery lesions by dipyridamole echocardiography. Comparison with positron emission tomography and quantitative arteriography Circulation, 1994, 89, 753-761.	1.6	83
220	Global alteration in perfusion response to increasing oxygen consumption in patients with single-vessel coronary artery disease Circulation, 1994, 90, 1696-1705.	1.6	73
221	Evaluation of regional myocardial systolic and diastolic function using ECC-gated Sestamibi scintigraphy. International Journal of Cardiovascular Imaging, 1993, 9, 49-55.	0.6	1
222	Non-invasive assessment of residual viability in postmyocardial infarction patients. International Journal of Cardiovascular Imaging, 1993, 9, 19-29.	0.6	0
223	Alteration in regulation of myocardial blood flow in one-vessel coronary artery disease determined by positron emission tomography. American Journal of Cardiology, 1993, 72, 538-543.	1.6	77
224	Does the myocardium become "stunned―after episodes of angina at rest, angina on effort, and coronary angioplasty?. American Journal of Cardiology, 1993, 71, 1045-1051.	1.6	26
225	Value of rest thallium-201/technetium-99m sestamibi scans and dobutamine echocardiography for detecting myocardial viability. American Journal of Cardiology, 1993, 71, 166-172.	1.6	220
226	Regional myocardial blood flow in stable angina pectoris associated with isolated significant narrowing of either the left anterior descending or left circumflex coronary artery. American Journal of Cardiology, 1993, 72, 990-994.	1.6	40
227	Residual coronary reserve despite decreased resting blood flow in patients with critical coronary lesions. A study by technetium-99m human albumin microsphere myocardial scintigraphy Circulation, 1993, 87, 330-344.	1.6	34
228	Myocardial blood flow distribution in patients with ischemic heart disease or dilated cardiomyopathy undergoing heart transplantation Circulation, 1993, 88, 509-522.	1.6	131
229	Prediction of reversible perfusion defects by quantitative analysis of post-exercise electrocardiogram-gated acquisition of technetium-99m 2-methoxyisobutylisonitrile myocardial perfusion scintigraphy. European Journal of Nuclear Medicine and Molecular Imaging, 1992, 19, 796-9.	2.1	9
230	The clinical usefulness of electrocardiogram-gated Tc-99 m methoxy-isobutyl-isonitrile images in the detection of basal wall motion abnormalities and reversibility of stress induced perfusion defects. International Journal of Cardiovascular Imaging, 1992, 8, 131-141.	0.6	12
231	Accuracy and safety of technetium-99m hexakis 2-methoxy-2-isobutyl isonitrile (Sestamibi) myocardial scintigraphy with high dose dipyridamole test in patients with effort angina pectoris: A multicenter study. Journal of the American College of Cardiology, 1991, 18, 1439-1444.	2.8	51
232	The hyperbolic relationship between systolic pressure-volume ratio and end-diastolic volume in man: A new approach to the non-invasive evaluation of left ventricular function. Journal of the American College of Cardiology, 1991, 17, A83.	2.8	0
233	Clinical significance of 99mTc-MIBI uptake defects at rest in noninfarcted male patients. Journal of the American College of Cardiology, 1991, 17, A251.	2.8	2
234	Noninvasive Quantitative Assessment of Segmental Myocardial Wall Motion Using Technetium-99m 2-Methoxy-Isobutyl-Isonitrile Scintigraphy. American Journal of Noninvasive Cardiology, 1990, 4, 22-28.	0.1	6

#	Article	IF	CITATIONS
235	Behavior of right and left ventricles during episodes of variant angina in relation to the site of coronary vasospasm Circulation, 1990, 81, 567-577.	1.6	15
236	Comparison of Dipyridamole-Echocardiography Test and Exercise Thallium-201 Scanning for Diagnosis of Coronary Artery Disease. American Journal of Noninvasive Cardiology, 1989, 3, 85-92.	0.1	19
237	Multiparametric approach to diagnosis of non-Q-wave acute myocardial infarction. American Journal of Cardiology, 1989, 63, 404-408.	1.6	30
238	Characterization of non-Q wave infarction by radioisotopic methods. European Journal of Nuclear Medicine and Molecular Imaging, 1986, 12, S51-S53.	2.1	0